Electronic Supplementary Information

Three-in-one is really better: Exploring sensing and adsorption properties in a newly designed metal-organic system incorporating copper(II) ion

Formula for calculating the percentage of Nitrobenzene fluorescence intensity quenching:

$$(I_o\text{-}I)/I_o \times 100\%$$

Where, I_o = initial fluorescence intensity,
I = intensity of CP (**1**) containing nitrobenzene solution.

Reference: (a) S. Pramanik, C. Zheng, X. Zhang, T. J. Emge and J. Li, *J. Am. Chem. Soc*., 2011, **133**, 4153; (b) D. Banerjee, Z. Hu and J. Li, *Dalton Trans*., 2014, **43**, 10668.

Stern-Volmer equation:

$$I_0/I = K_{SV}[A] + 1$$

Where, I_0 = fluorescent intensity of CP (**1)** before the addition of the analyte
I = fluorescent intensity after the addition of the respective analyte
K_{SV} = Stern-Volmer constant
[A] = molar concentration of the analyte (M^{-1}).

Topological analysis for CP (1)

1:C7 Cu N2 O S

Topology for Cu1

Atom Cu1 links by bridge ligands and has

Common vertex with					R(A-A)	
Cu 1	-0.0054	0.6154	-0.0523	(0 1 0)	3.004A	1
Cu 1	0.0054	0.1154	-0.4477	(0 0-1)	5.416A	1
Cu 1	0.0054	0.1154	0.5523	(0 0 0)	5.416A	1

Structural group analysis

Structural group No 1

Structure consists of layers (1 0 0) with Cu

Coordination sequences

Cu1: 1 2 3 4 5 6 7   8   9 10

Num   3 6 9 12 15 18 21 24 27 30

Cum   4 10 19 31 46 64 85 109 136 166

TD10=166

Vertex symbols for selected sublattice

Cu1 Point symbol:{6^3}

Extended point symbol:[6.6.6]

Point symbol for net: {6^3}

3-c net; uninodal net

Topological type: hcb; Shubnikov hexagonal plane net/(6,3)

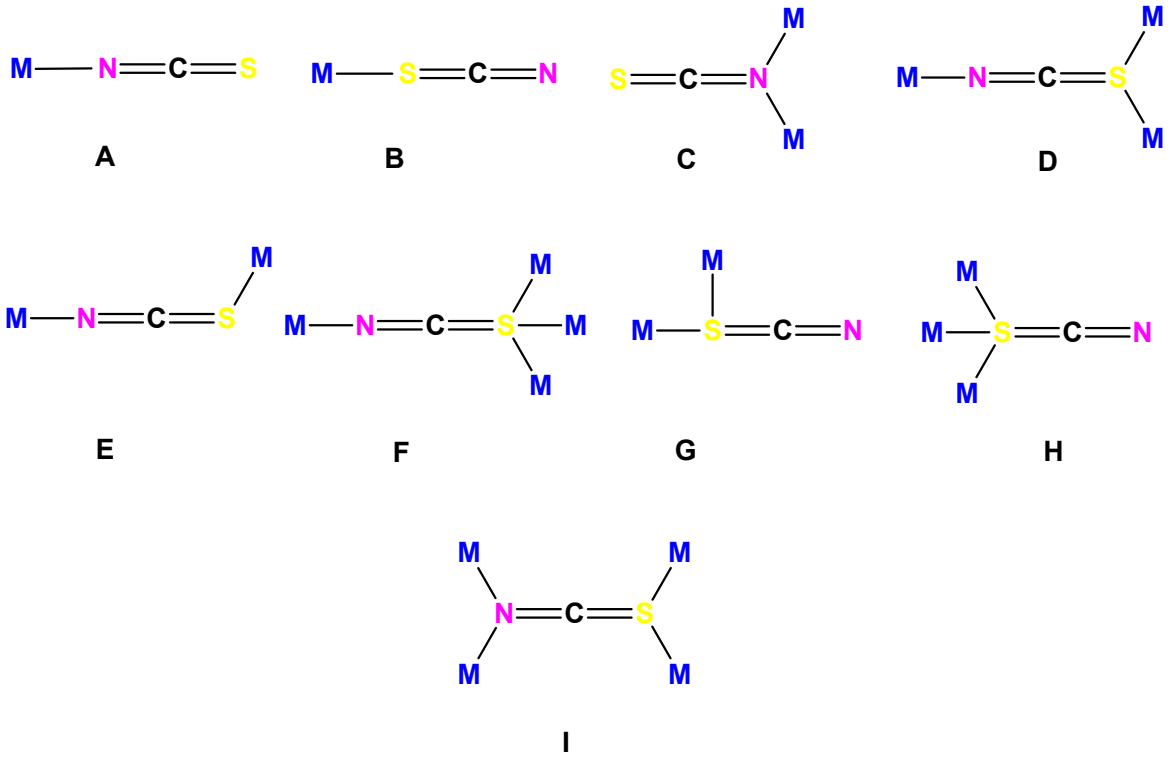

Scheme S1 Important coordination modes of NaSCN ligand.

Table S1 Selected bond lengths (Å) and bond angle (degree) for CP (**1**)

Cu1–Cu1	3.0041
Cu1–O1	1.917(3)
Cu1–O1	1.930(3)
Cu1–N1	1.980(4)
Cu1–N2	1.915(4)
N1–Cu1–O1	158.83(14)
N1–Cu1–O1	81.85(14)
N2Cu1O1	99.46(15)
N2–Cu1–O1	169.68(15)
N2–Cu1–N1	100.41(16)
C1–O1–Cu1	138.8(3)
C1–O1–Cu1	115.3(3)
C2–N1–Cu1	113.5(3)
C6–N1–Cu1	127.7(3)
C7–N2–Cu1	168.7(4)

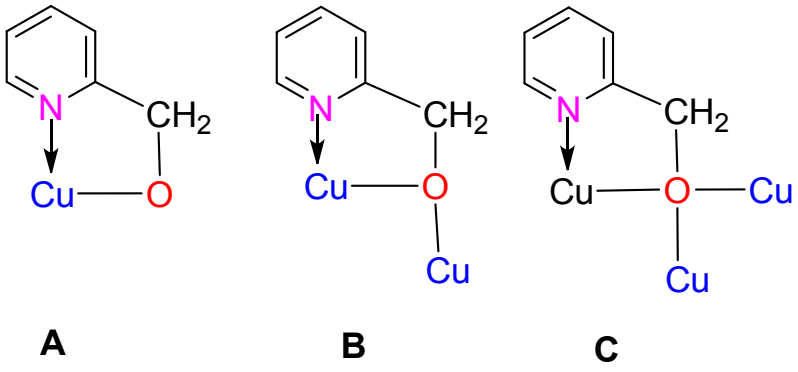

Scheme S2. Important coordination modes of hmp ligand.

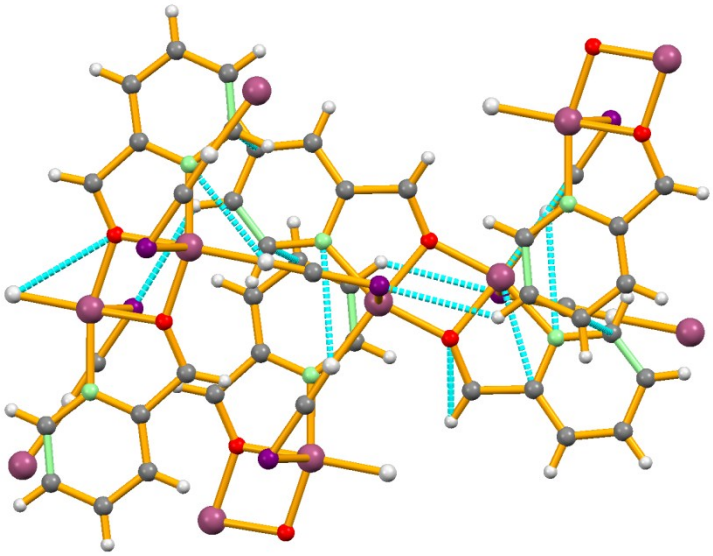

Figure S1: Formation of 3-D supramolecular network due to various supramolecular interaction in CP (**1**).

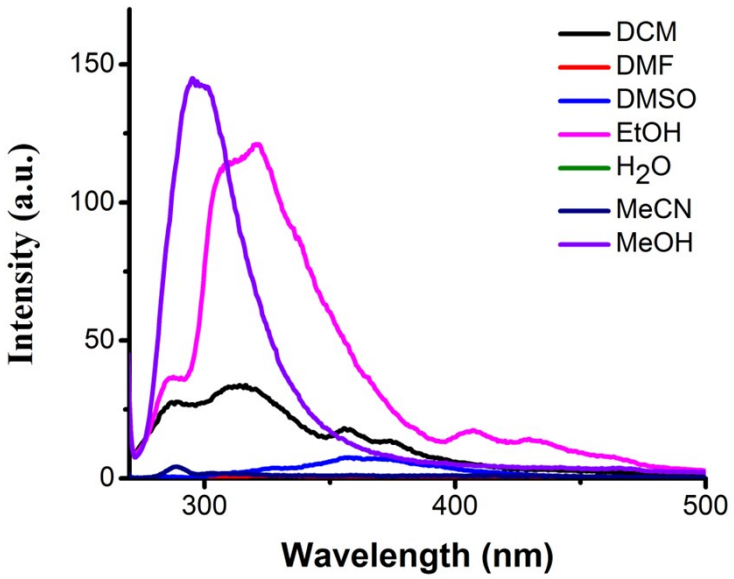

Figure S2: Emission spectrum of CP (**1**) dipped in different solvents upon excitation at 250 nm.

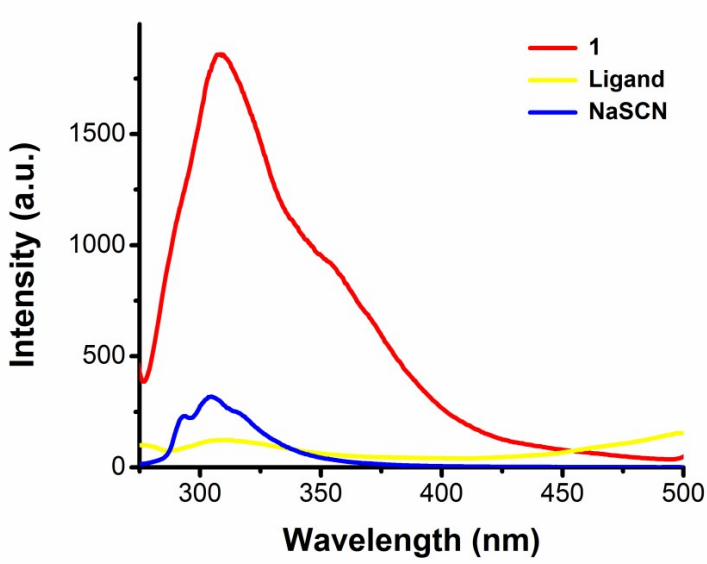

Figure S3: Emission spectrum of CP (**1**), hmpH and NaSCN ligand in methanol upon excitation at 250 nm.

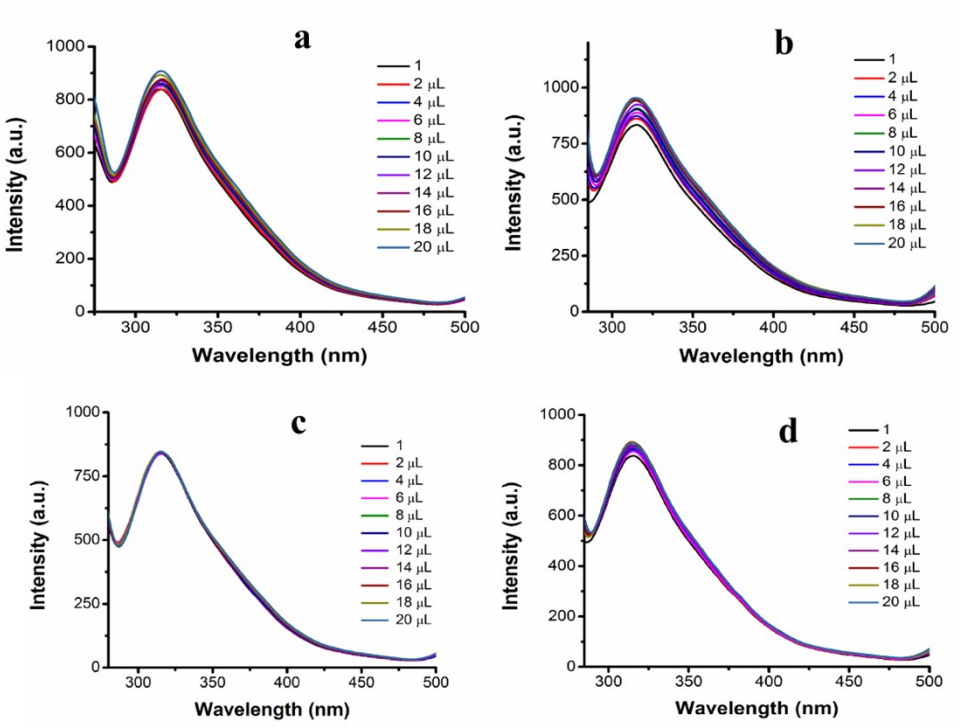

Figure S4: The change in fluorescence intensity of CP (**1**) upon incremental addition of DNT (a), m-DNB (b), NT (c) and p-DNB (d) solution.

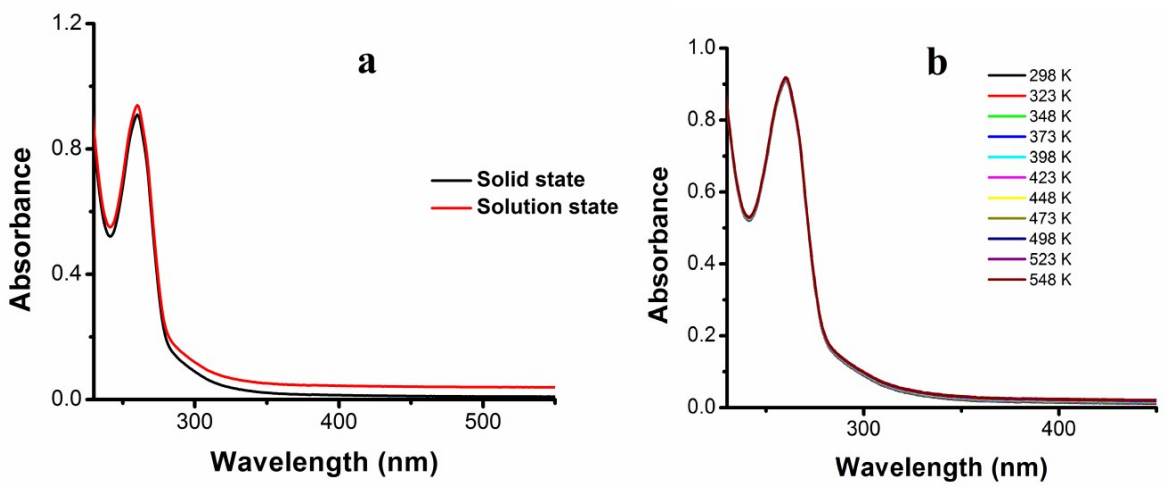

Figure S5: Solid and solution state (a), temperature dependent (b) UV-Visible spectra of CP (**1**) in methanol.

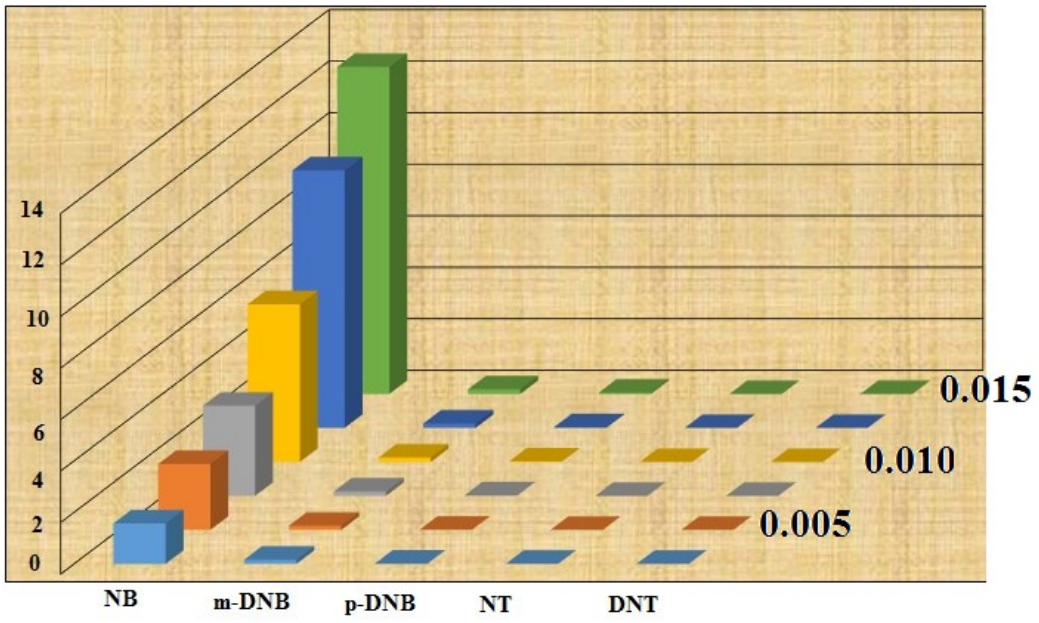

Figure S6: 3-D representation of Stern–Volmer (SV) plot for various nitro aromatic analytes.

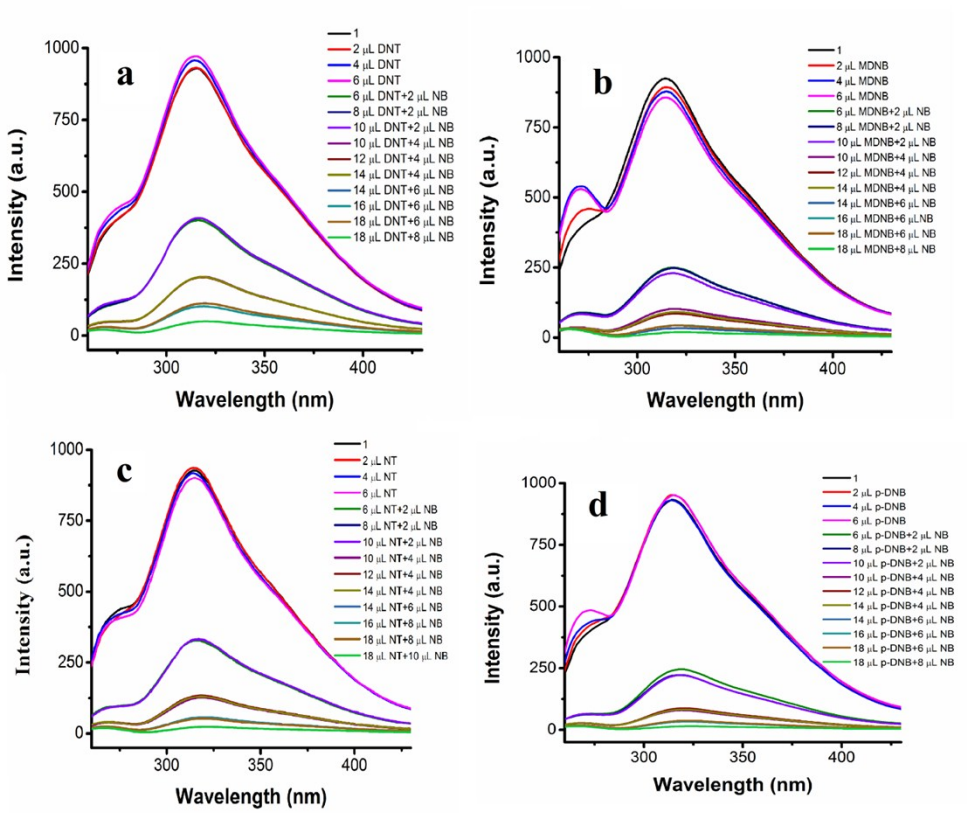

Figure S7: The change in fluorescence intensity of CP (**1**) upon addition of DNT (a), m-DNB (b), NT (c) and p-DNB (d) followed by NB.

Table S2: - HOMO and LUMO energies calculated for nitroaromatics analytes and hmpH (ligand) at B3LYP/6- 31G* level of theory.

Compound	HOMO	LUMO	Band Gap
p-NB	-8.4592	-4.3364	4.1228
m-NB	-8.42899	-3.93558	4.4934
d-NT	-7.99661	-3.79708	4.1995
NT	-7.60395	-3.09151	4.5124
NB	-7.63606	-2.94917	4.6868
Ligand	-6.93727	-1.55662	5.3806

Table S3: The Vapor pressure and reduction potential of common explosives and selected analytes

Analytes	**Vapor Pressure (in mmHg,# at 25 °C)**	**Reduction Potential[(a)] (in V vs SCE)**
Nitrobenzene (NB)16	0.2416	-1.15
1,3-Dinitrobenzene (m-DNB)17	8.82×10^{-4}	-0.9
1,4-Dinitrobenzene (p-DNB)16	2.406×10^{-5}	-0.7
2-Nitrotoluene (NT)16	0.1602	-1.2
2,4-Dinitrotoluene (2,4-DNT)16	1.44×10^{-4}	-1.0

[#]1 mmHg = 1.2468×10^3 ppm

[(a)]Debasis Banerjee, Zhichao Hu, and Jing Li, *DaltonTrans*., 2014, **43**, 10668.

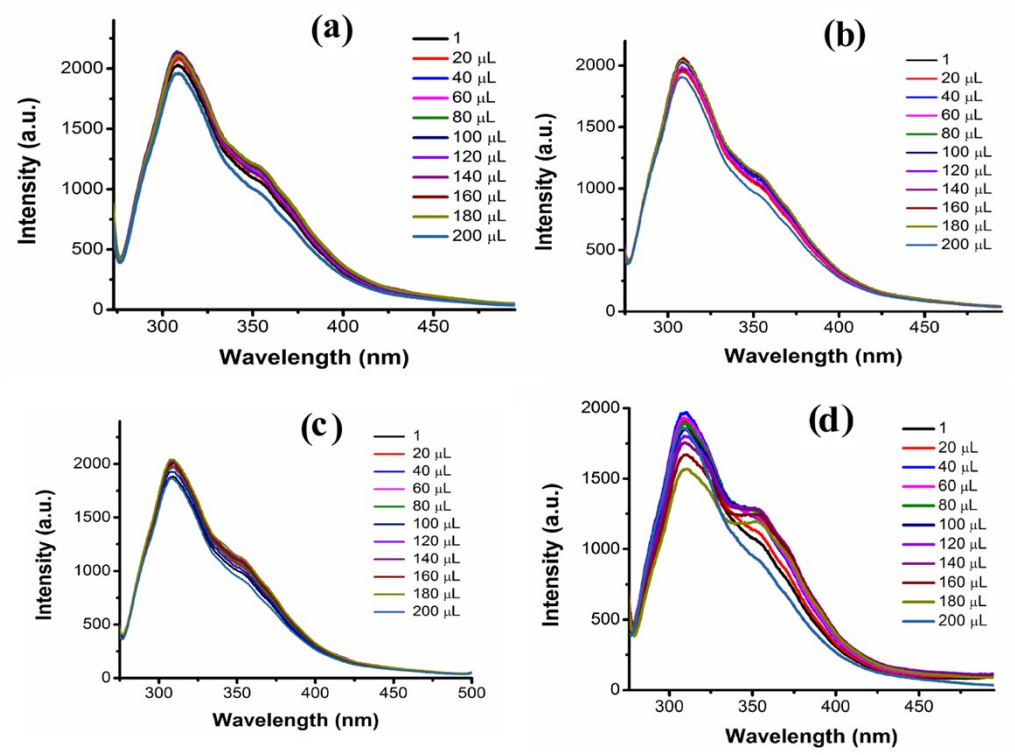

Figure S8: Emission spectrum of CP (**1**) upon incremental addition of 1mM solution of K^{+} (a), Ca^{2+}(b), Mg^{2+} (c) and Cr^{3+} (d) metal ions in methanol.

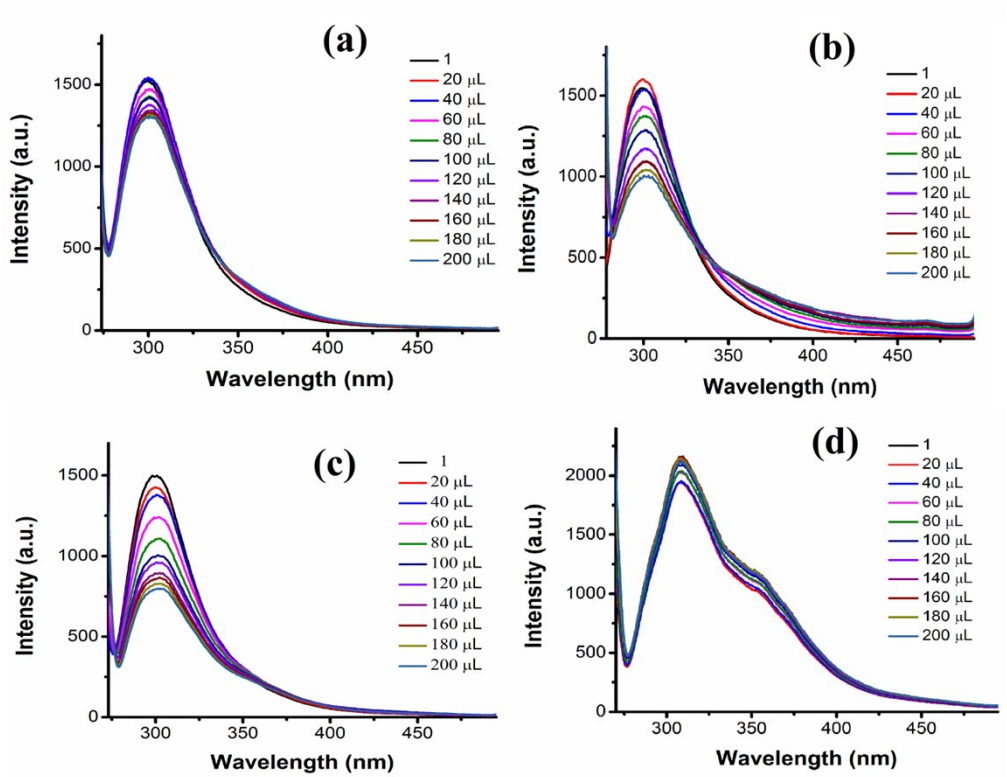

Figure S9: Emission spectrum of CP (**1**) upon incremental addition of 1mM solution of Mn^{2+}(a), Co^{2+}(b), Ni^{2+}(c) and Cu^{2+}(d) metal ions in methanol.

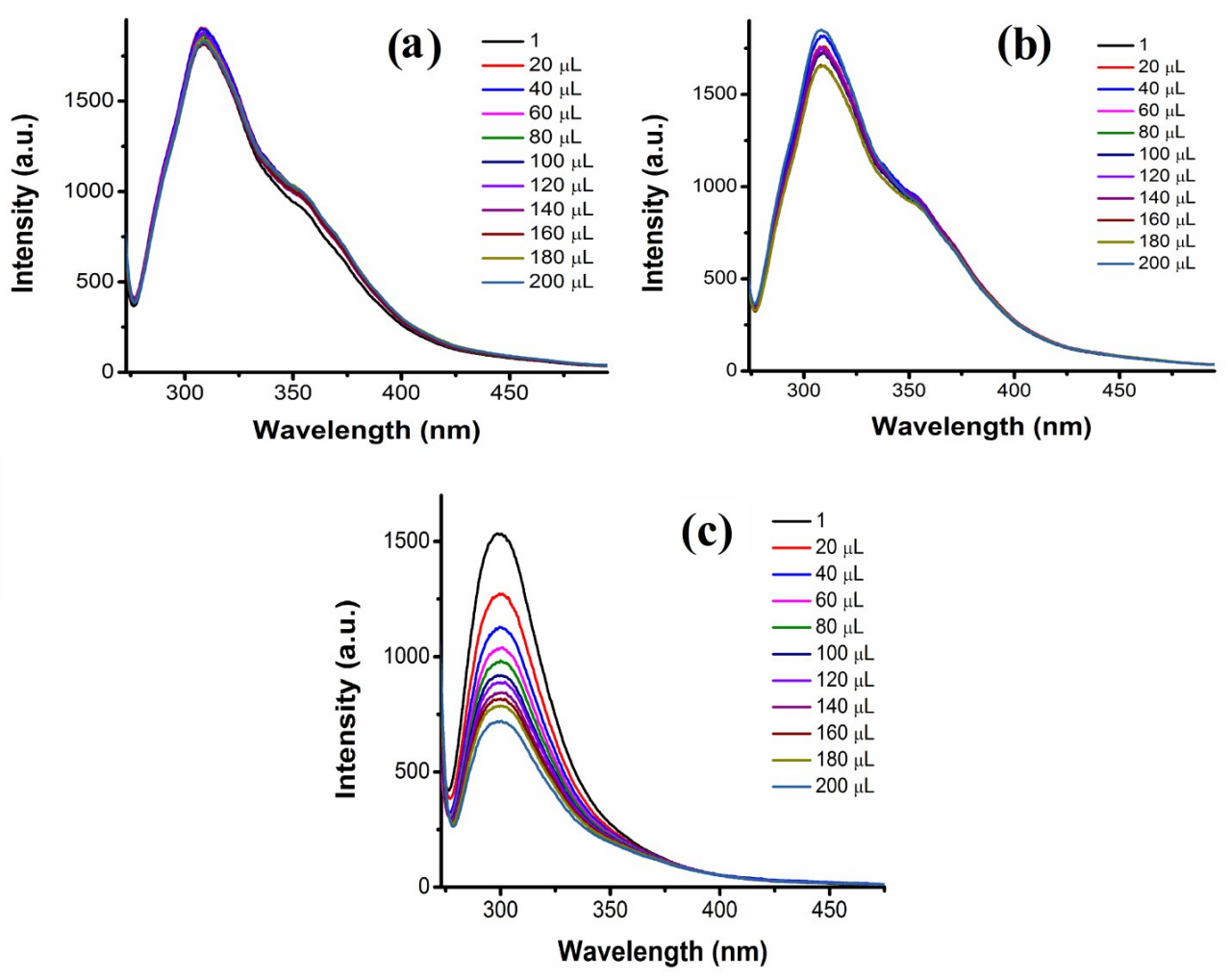

Figure S10: Emission spectrum of CP (**1**) upon incremental addition of 1mM solution of Zn^{2+} (a), Hg^{2+} (b) and Pb^{2+} (c) metal ions in methanol.

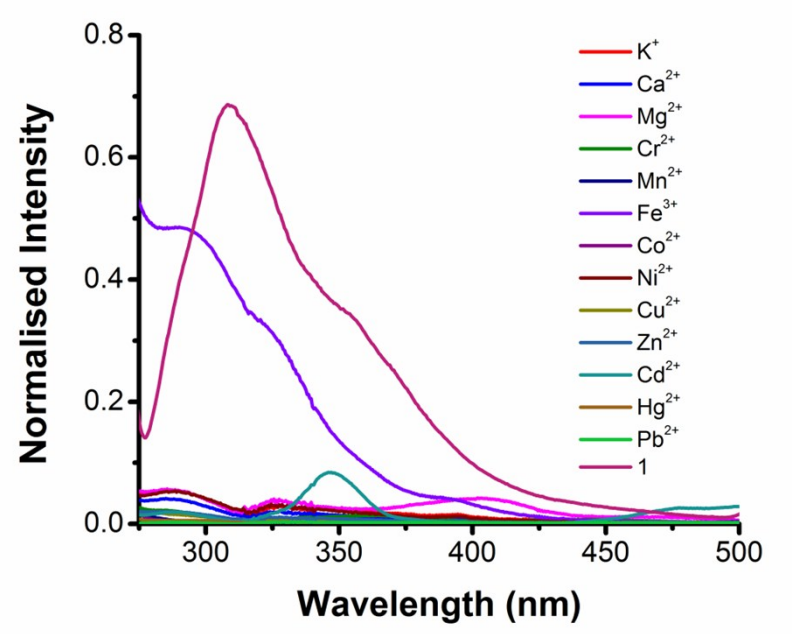

Figure S11: Spectral overlap between normalized emission spectra of CP (**1**) (λex = 250 nm) and normalized absorbance spectra of the metal ions.

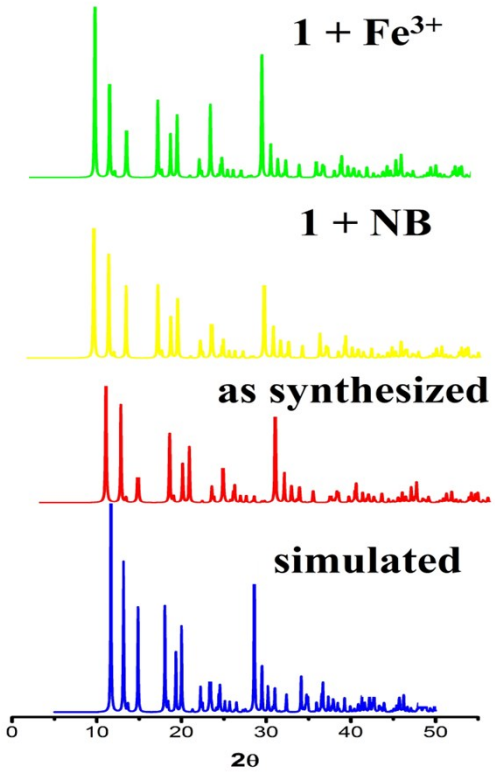

Figure S12: PXRD patterns of CP (**1**): simulated (blue) as-synthesized (red), after immersion in NB (yellow) and Fe^{3+}solution (green).

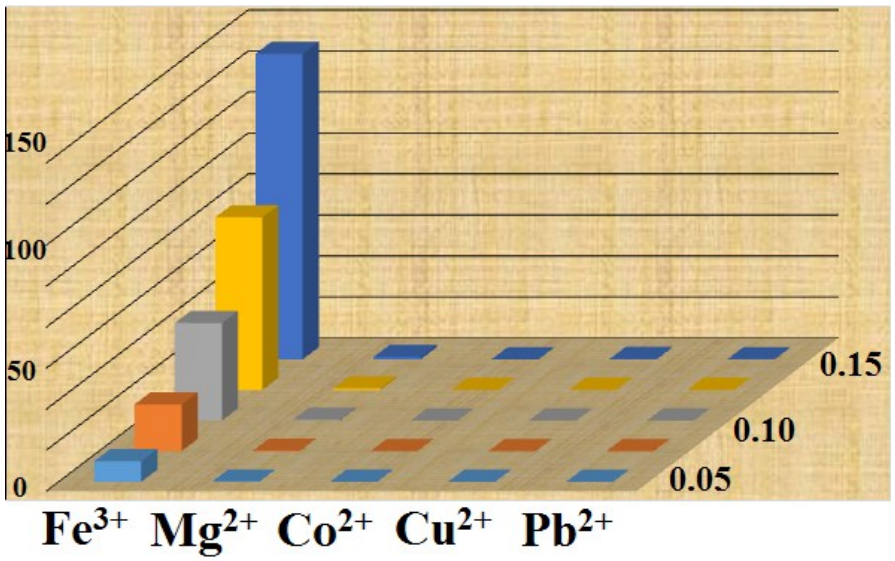

Figure S13 3-D representation of Stern–Volmer (SV) plot for various metal ions.

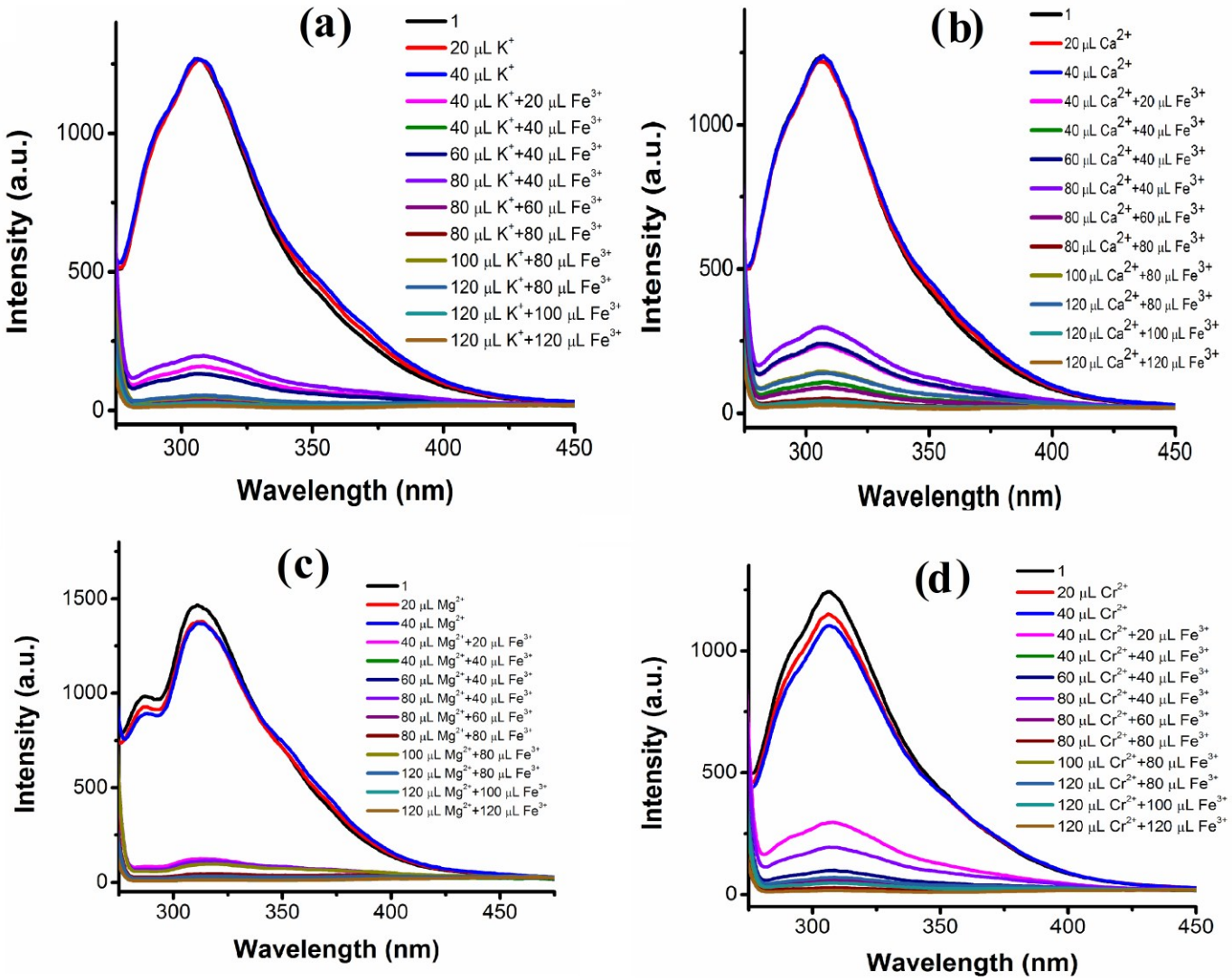

Figure S14: The change in fluorescence intensity of CP (**1**) upon addition of K^+ (a), Ca^{2+} (b), Mg^{2+} (c) and Cr^{3+} (d) solution followed by Fe^{3+} solution respectively in methanol.

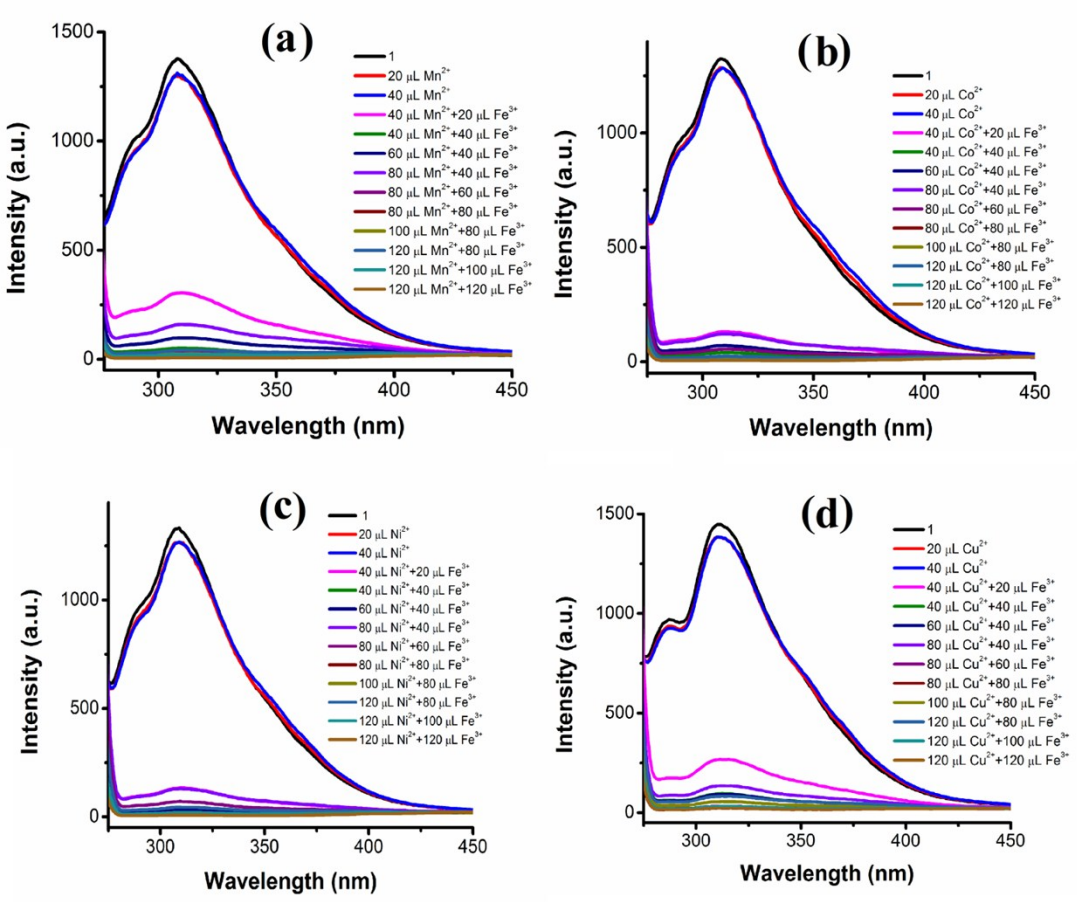

Figure S15: The change in fluorescence intensity of CP (**1**) upon addition of Mn^{2+} (a), Co^{2+} (b), Ni^{2+} (c) and Cu^{2+} (d) solution followed by Fe^{3+} solution respectively in methanol.

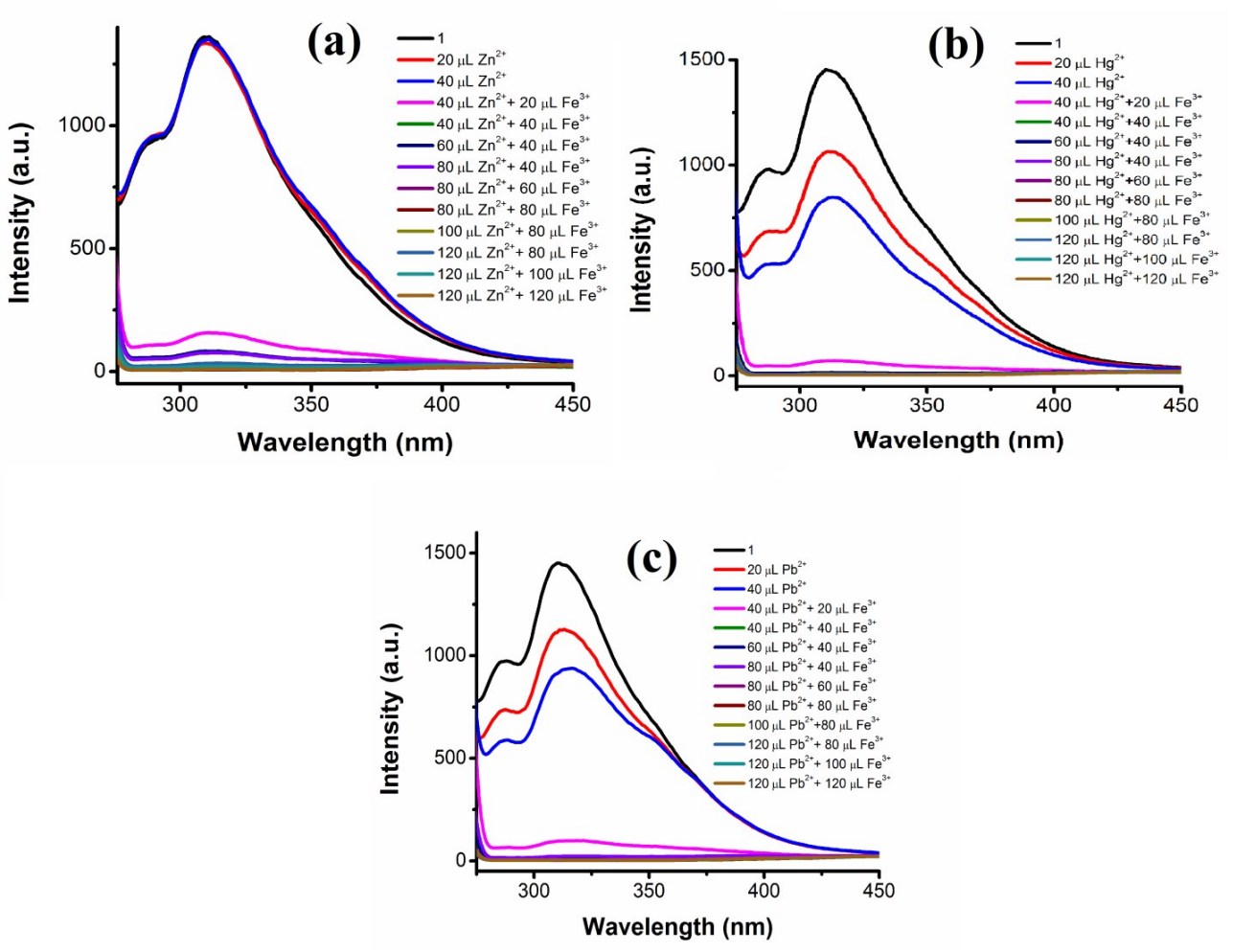

Figure S16: The change in fluorescence intensity of CP (**1)** upon addition of Zn^{2+} (a), Hg^{2+} (b), and Pb^{2+} (c) solution followed by Fe^{3+} solution respectively in methanol.

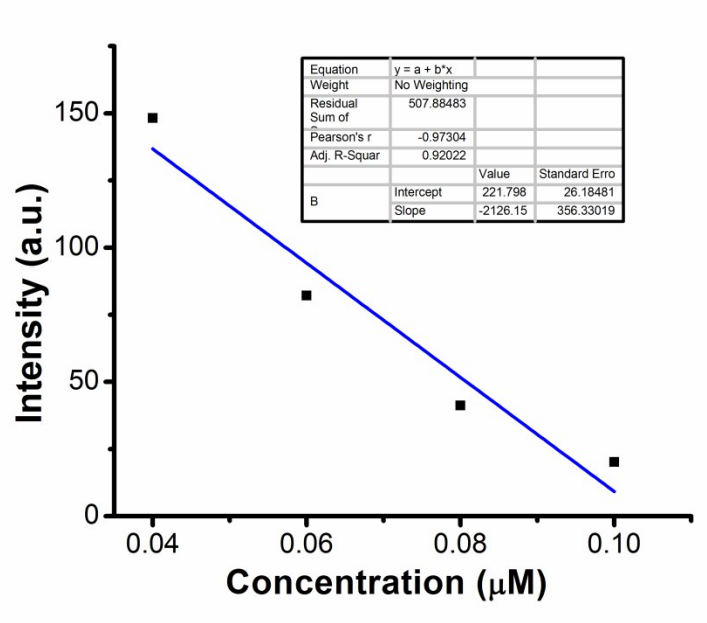

Figure S17: Linear region of fluorescence intensity of CP (**1**) upon addition of Fe^{3+} in methanol (20 – 200 μL, 1 mM stock solution) (upon λ_{ex}= 250nm) (R^2= 0.92).

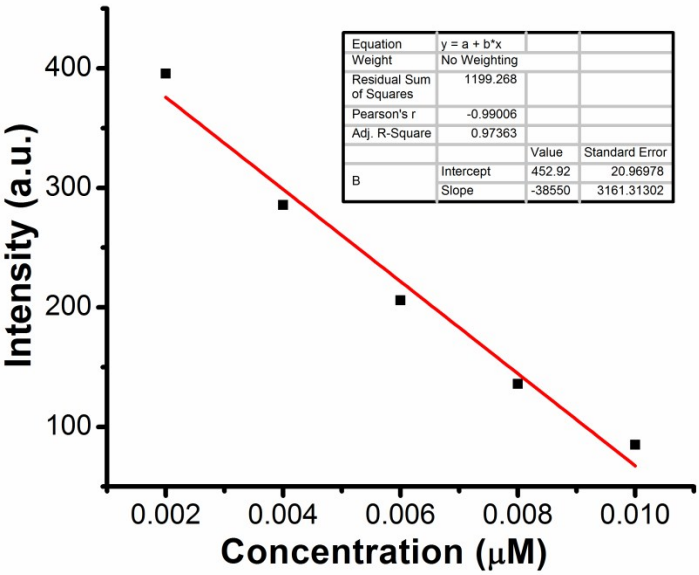

Figure S18: Linear region of fluorescence intensity of CP (**1**) upon addition of NB in methanol (2 – 20 μL, 2 mM stock solution) (upon λ_{ex}= 250nm) (R^2= 0.97).

Calculation of standard deviation:

Table S4: Standard deviation for CP (**1**).

Blank Readings (only CP)	**Intensity of CP (1)**
Reading 1	907.5
Reading 2	910.2
Reading 3	911.1
Reading 4	904.6
Reading 5	914.4
Standard Deviation (σ)	**3.7**

Calculation of Detection Limit:

Table S5: Detection limit calculation of CP (**1**) for NB

Compound 1	**Slope from Graph (m)**	**Detection limit (3σ/m)**	
		µM	**ppb**
1	38550	2.8×10^{-4}	0.03531

Table S6: Detection limit calculation of CP (**1**) for Fe^{3+}

Compound 1	**Slope from Graph (m)**	**Detection limit (3σ/m)**	
		µM	**ppb**
1	2126.15	5.2×10^{-3}	0.8434

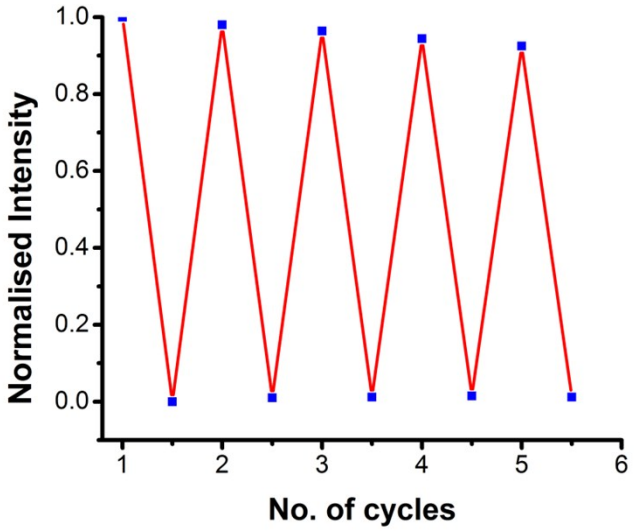

Figure S19: Recyclability test of CP (**1**), the upper dots represent the initial luminescence intensity and the lower dots represent the intensity upon addition of NB solution.

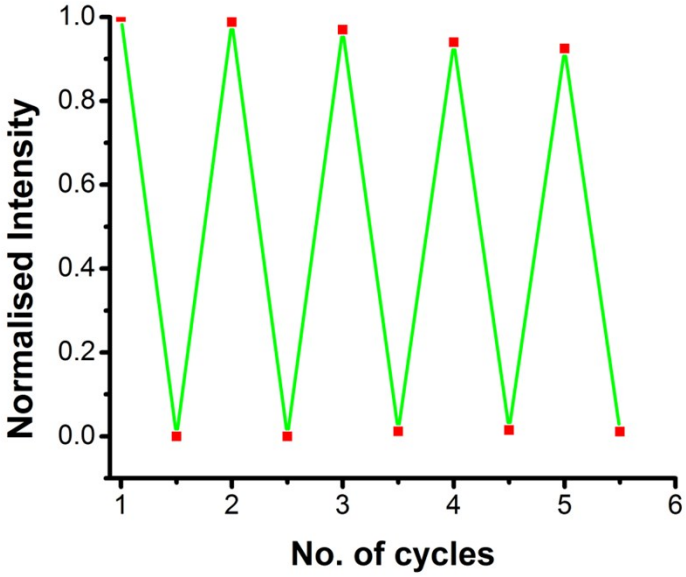

Figure S20: Recyclability test of CP (**1**), the upper dots represent the initial luminescence intensity and the lower dots represent the intensity upon addition of Fe^{3+} solution.

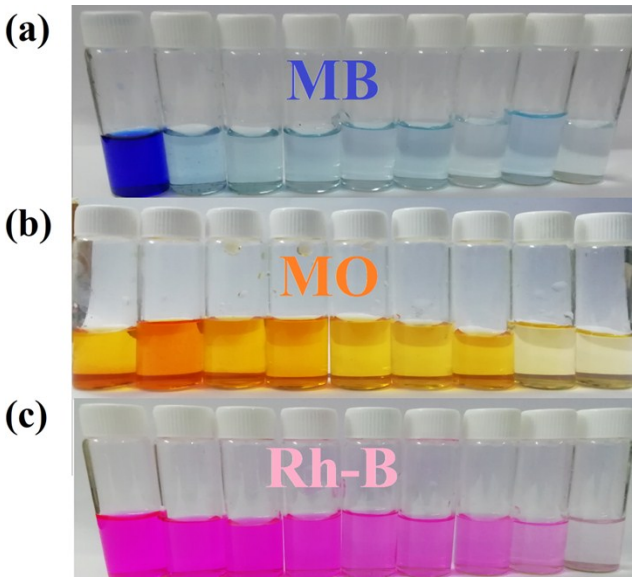

Figure S21: The decolorization of different dyes with increasing time MB (a), MO (b), Rh-B (c) in presence of CP (**1**).

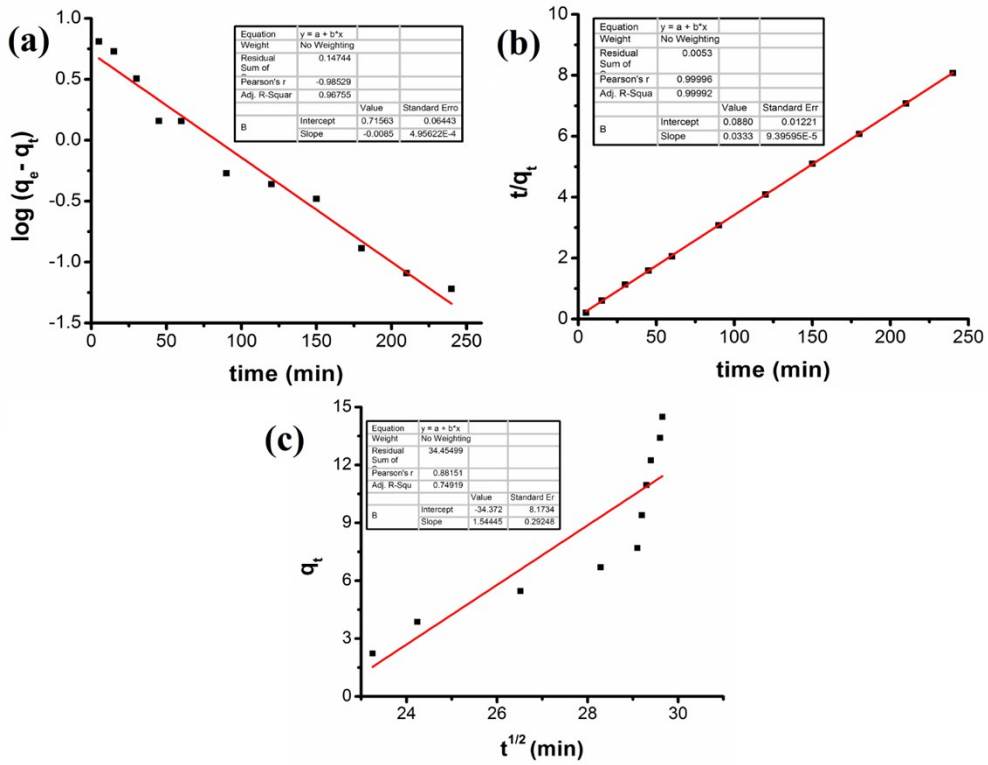

Figure S22: The adsorption of MB onto CP (**1**) using pseudo-first-order (a), pseudo-second-order (b)and intra particle (c) kinetics model.

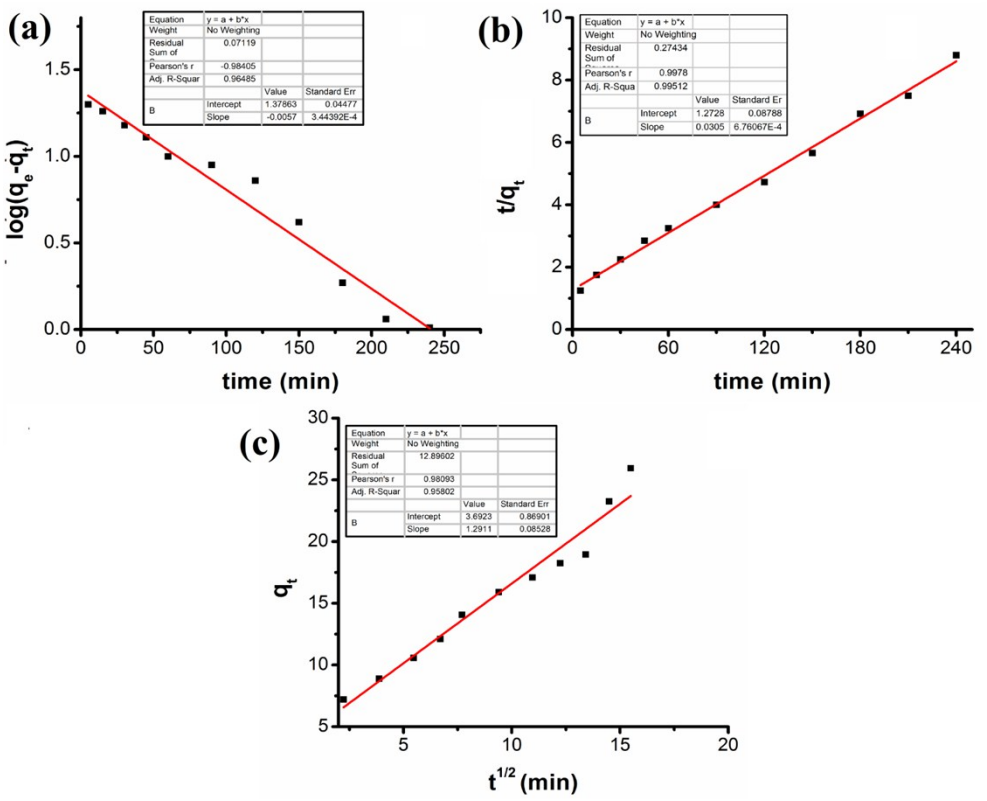

Figure S23: The adsorption of MO onto CP (**1**) using pseudo-first-order (a), pseudo-second-order (b), and intra particle (c) kinetics model.

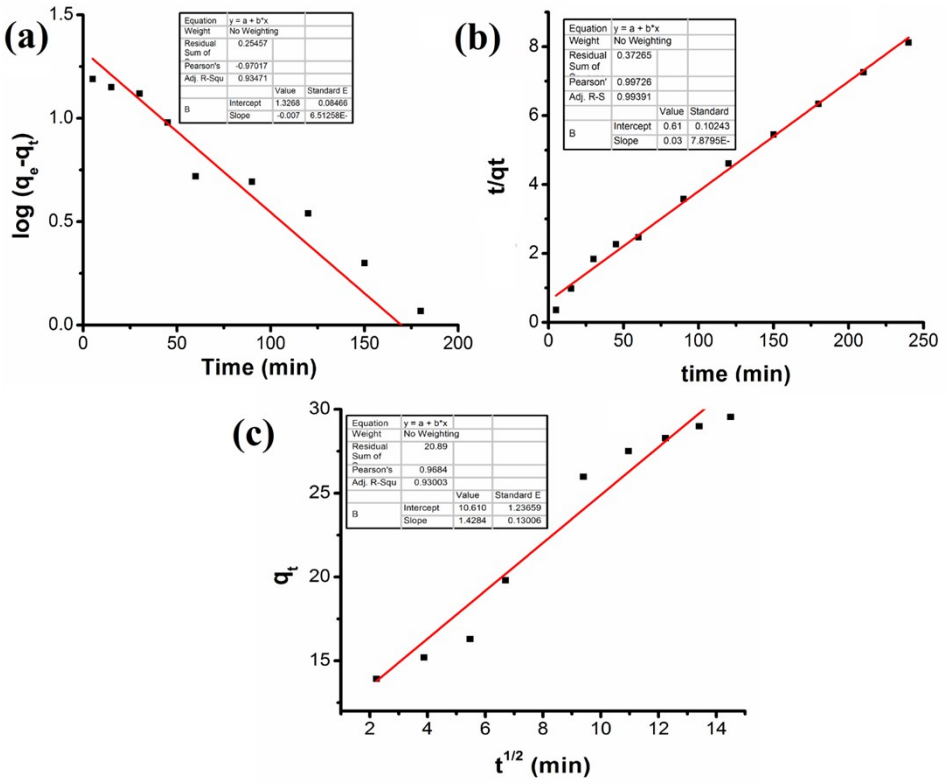

Figure S24: The adsorption of Rh-B onto CP (**1**) using pseudo-first-order (a), pseudo-second-order (b), and intra particle (c) kinetics model.